Pharmaceutical Research, Vol. 4, No. 5, 1987

Research Article

Diketopiperazine Formation, Hydrolysis, and Epimerization of the New Dipeptide Angiotensin-Converting Enzyme Inhibitor RS-10085

Leo Gu[1,2] and Robert G. Strickley[1]

Received April 29, 1987; accepted June 18, 1987

The degradation kinetics, products, and mechanisms of RS-10085(**1**), 2-[2-(1-ethoxycarbonyl)-3-phenylpropyl]amino-1-oxopropyl]-6,7-dimethoxy-1,2,3,4-tetrahydroisoquinoline-3-carboxylic acid(S,S,S), in aqueous solution were investigated at 40, 60, and 80°C from pH 1 to pH 13. Pseudo-first-order kinetics were observed throughout the pH range studied and the log(rate)–pH profiles reflected four kinetic processes (k_o, k'_o, k''_o, and k_{OH}) as well as the two *p*Ka's of **1**. Excellent (>98%) mass balance was obtained through products **2–5**. At pH 4 or below, intramolecular cyclization leading to diketopiperazine **5** accounted for greater than 93% of the observed neutral- or water-catalyzed processes (k_o and k'_o). At pH levels greater than 5, hydrolysis giving **2** predominated and was responsible for the observed neutral- or water-catalyzed (k''_o) and specific base-catalyzed (k_{OH}) kinetic processes. Some epimerization leading to the S,S,R drug isomer (**4**) was also observed at pH levels greater than 7. The relative acidity of the protons at the three chiral centers of **1** was qualitatively compared and was used to explain the observed specificity in epimerization.

KEY WORDS: angiotensin-converting enzyme (ACE) inhibitor; RS-10085; degradation; kinetics; products; diketopiperazine; peptides.

INTRODUCTION

RS-10085 (**1**) (Fig. 1), 2-[2-[(1-ethoxycarbonyl)-3-phenylpropyl]amino-1-oxopropyl]-6,7-dimethoxy-1,2,3,4-tetrahydro-isoquinoline-3-carboxylic acid(S,S,S), belongs to a class of *N*-carboxyalkyl dipeptide analogues (1) that has recently been discovered to be potent angiotensin-converting enzyme (ACE) inhibitors (2,3). Like many of these dipeptide ACE inhibitors, RS-10085 is being developed as the ester derivative of the biologically active diacid form RS-10029 (**2**) (Fig. 1) for better oral bioavailability (1). The hydrochloride salt was selected as the drug form for development for its crystallinity. In this paper, the kinetics, products, and mechanisms of the thermal degradation of RS-10085 in aqueous solution are explored in order to facilitate the design of a suitable intraveneous (iv) formulation for toxicological and clinical studies.

EXPERIMENTAL

Materials

RS-10085 (**1**), RS-10029 (**2**), RS-10029 diketopiperazine (**3**), compound **4** (S,S,R isomer of **1**) and RS-10085 diketopiperazine (**5**) were obtained from the Institute of Organic Chemistry, Syntex Research. High-performance liquid chromatographic (HPLC)-grade acetonitrile and tetrahydrofuran and nanopure water were used to prepare the mobile phase. All other chemicals were analytical grade and were used as received.

Instrumentation

A Radiometer Model PHM64 Research pH meter equipped with a Radiometer Model GK2410C combination electrode was used to measure the pH of the solution. HPLC was performed using a Spectra-Physics Model 3500 pump equipped with a Kratos 757 variable-wavelength UV detector, a Micromeritics 728 autosampler, and a Spectra-Physics 4100 computing integrator.

Dissociation Constants (*p*Ka)

Three hundred and fifty milligrams of drug was added to 35.0 ml of water (0.0188 mol of **1**) in a thermal-jacketed beaker equilibrated to the desired temperature. With constant stirring the drug solution was titrated with an 0.083 *M* standard KOH solution. The pH was measured and the *p*Ka values were determined using the Noyes' method (4).

HPLC Method

The reverse-phase HPLC method employed an Altex Ultrasphere–ODS 5-μm column and a mobile phase of ammonium phosphate buffer (0.05 *M*, pH 2.0)/acetonitrile/tetrahydrofuran (55/35/10). The detection wavelength was 220 nm and the detector sensitivity was 0.05 AUFS. The lin-

[1] Institute of Pharmaceutical Sciences, Syntex Research, Palo Alto, California 94304.

[2] To whom correspondence should be addressed.

0724-8741/87/1000-0392$05.00/0

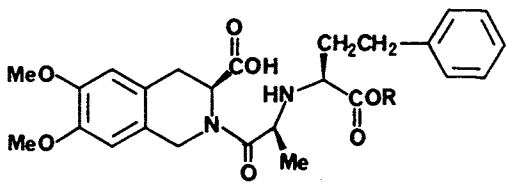

1, RS-10085(S,S,S); R= Et
2, RS-10029(S,S,S); R= H

Fig. 1. Structures of RS-10085 (1) and RS-10029 (2).

earity of the method was demonstrated in the range of 0.05 to 5.5 μg compound injected using either peak area or peak height measurement (r = 0.999). The stability specificity of the method was supported by the complete disappearance of 1 when totally degraded samples were injected.

Kinetic Methods

Acetate, phosphate, and carbonate buffer solutions containing 0.010 M total buffer concentration were freshly prepared before use and KCl was added to adjust the total ionic strength to 0.10 M. The pH of each solution was measured at the reaction temperature. For very acidic and basic solutions, aqueous HCl and KOH solutions were used to obtain the desired pH.

In a typical kinetic experiment, 1.5-ml aliquots of the buffer solution containing 20–50 μg/mL of 1 were transferred to pretreated 2-ml Type I amber glass ampoules. The ampoules were then flame-sealed and stored in a 40, 60, or 80°C oven until predetermined time periods when the ampoules were removed and quenched to 0°C in an ice bath. The samples were allowed to warm to room temperature before assaying by HPLC.

RESULTS AND DISCUSSION

At least three major forms of 1, i.e., the cation (1c), zwitterion (1z), and anion (1a), exist in aqueous solution reflecting the pKa$_1$, and pKa$_2$ of 1 (Scheme I).

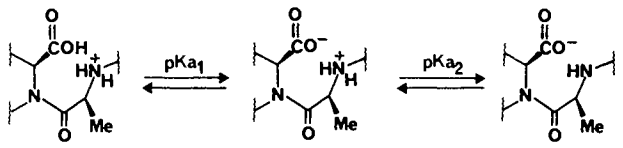

1c Scheme I 1z 1a

The effect of temperature on these two pKa values was determined by titration and the results are summarized in Table I. The values of the carboxylic acid pKa were virtually identical throughout the temperature range of 25 to 80°C as expected, whereas the amino pKa decreased as the temperature increased, consistent with that expected for a typical amine (5). At 25°C, the two pKa values of 1 compare very well with that of enalapril (1), which is a structurally related ACE inhibitor. The different temperature effects on the two pKa's of 1 further confirm the assigned charges on the various species shown in Scheme I.

Table I. Effect of Temperature on the Dissociation Constants (pKa) of 1[a]

Temperature (°C)	pKa$_1$	pKa$_2$
80	3.02	4.74
60	3.07	4.94
40	3.05	5.11
25	3.03	5.40

[a] Obtained by the titration method; see Experimental for details.

Kinetics

The aqueous stability of RS-10085 (1) was studied in buffer solutions from pH 1 to pH 13 at 40, 60, and 80°C. The kinetics of the degradation were analyzed by a stability-specific HPLC method (see Experimental) and were found to be strictly first-order to four half-lives. Since very low buffer concentrations were used (0.01 M), no correction was made for possible buffer catalysis.

Typical first-order plots at 40°C and pH 2, 5, and 10 are given in Fig. 2. The influence of pH on the decomposition kinetics of 1 can best be depicted by the log (rate)–pH profile shown in Fig. 3, in which the logarithm of the observed rate constants (k_{obs}) is plotted against pH. Although other kinetically competent systems are not ruled out, the shape of the rate profiles in Fig. 3 indicates the occurrence of neutral- or water-catalyzed processes for the cation 1c (k_o) and the zwitterion 1z (k'_o) and neutral- or water-catalyzed (k''_o) and specific-base catalyzed (k_{OH}) processes for the anion 1a according to the following rate expression:

$$\text{rate} = k_{obs}[1]_t \quad (1)$$

and

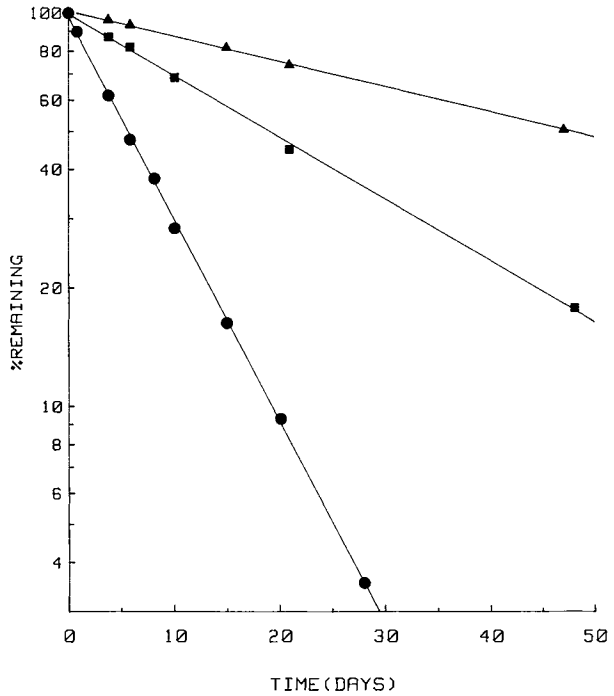

Fig. 2. Pseudo-first-order kinetics of the degradation of 1 in aqueous solution at 40°C: (a) pH 2.0 (●), (b) pH 5.0 (▲), and (c) pH 9.2 (■).

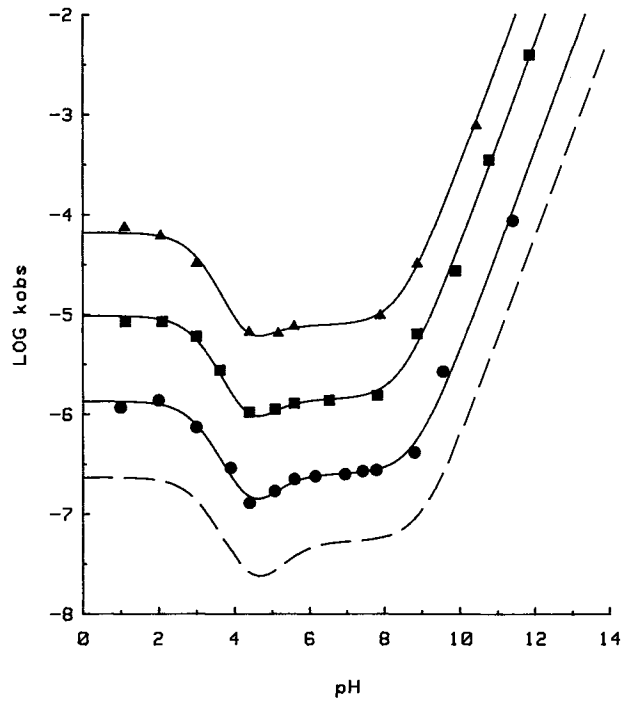

Fig. 3. Log(rate)–pH profiles for the degradation of 1 in aqueous solution at 40°C (●), 60°C (■) and 80°C (▲). The solid lines are the nonlinear regression fit using Eq. (2). The dashed line is the calculated log(rate)–pH profile at 25°C using the rate data (Table II) and the activation parameters (Table III).

$$k_{obs} = k_o[a_H^2/(Ka_1a_H + a_H^2 + Ka_1Ka_2)] + k'_o[Ka_1a_H/(Ka_1a_H + a_H^2 + Ka_1Ka_2)] + (k''_o + k_{OH}a_{OH})[Ka_1Ka_2/(Ka_1a_H + a_H^2 + Ka_1Ka_2)] \quad (2)$$

where $[1]_t$ is the total concentration of the drug, $a_H^2/(Ka_1a_H + a_H^2 + Ka_1Ka_2)$, $Ka_1a_H/(Ka_1a_H + a_H^2 + Ka_1Ka_2)$, and $Ka_1Ka_2/(Ka_1a_H + a_H^2 + Ka_1Ka_2)$ are, respectively, the fractions of **1c**, **1z**, and **1a**, and a_H and a_{OH} are, respectively, the hydrogen ion and hydroxide ion activity at the reaction temperature. Values for various apparent rate constants at different temperatures were determined according to Eq. (2) using the *p*Ka values listed in Table I and a nonlinear regression analysis method (6). The solid curves drawn in Fig. 3 were constructed from the apparent rate constants summarized in Table II. The excellent agreement between the experimental results and those calculated from Fig. 3 indicates that Eq. (2) adequately describes the observed pH effect on the degradation kinetics of **1**.

All the apparent rate constants listed in Table II were found to obey the Arrhenius equation (Fig. 4). The corresponding activation energies, entropies, and enthalpies derived are summarized in Table III. The rate constants at 25°C obtained by extrapolation were substituted into Eq. (2), affording the pH dependence on the rate of degradation at 25°C (dashed line in Fig. 3). The results predict a 2-month shelf life at 25°C at the pH of maximum stability, pH 4.5.

Product Distribution and Mechanism of the Degradation

In addition to product **2** due to ester hydrolysis, three additional products, **3** (diketopiperazine analogue of **2**), **4** (S,S,R drug isomer), and **5** (diketopiperazine analogue of **1**), were identified (Scheme II). An HPLC chromatogram showing the separation of the degradation product peaks and the drug peak using authentic samples is given in Fig. 5. No R,S,S drug isomer which eluted between peak **4** and peak **1** (not shown) was detected. Although an authentic sample of S,R,S drug isomer is not available at the present time, the excellent peak shape and the baseline separation of **4** in the degraded sample solutions (not shown) suggest that the S,R,S drug isomer is not formed under the reaction condition used.

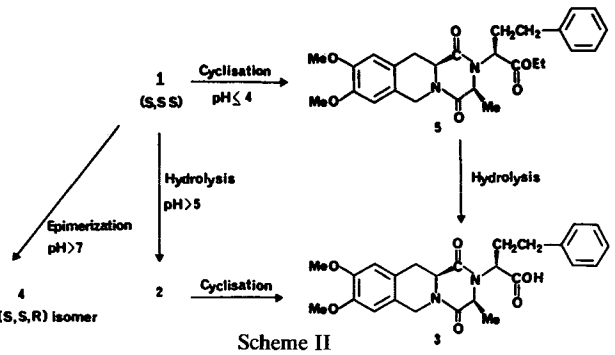

Scheme II

The material balance of the reaction determined using HPLC response factors of products **2**–**5** was found to be excellent and exceeded 98% under all conditions studied. The distribution of these products was similar at different temperatures but depended strongly on the pH of the solution. Figure 6 shows such a dramatic pH dependence on product distribution at 40°C and about 50% drug remaining. Thus at pH levels equal to or below 4, the diketopiperazine

Table II. Effect of Temperature on the Apparent Rate Constants for the Degradation of **1** in Aqueous Solution

Temperature (°C)	Rate constant[a]			
	k_0 (sec^{-1})	k'_0 (sec^{-1})	k''_0 (sec^{-1})	k_{OH} (M^{-1} sec^{-1})
80	6.86×10^{-5}	3.29×10^{-6}	7.93×10^{-6}	1.20×10^{-1}
60	1.01×10^{-5}	5.83×10^{-7}	1.42×10^{-6}	5.05×10^{-2}
40	1.41×10^{-6}	7.46×10^{-8}	2.54×10^{-7}	1.40×10^{-2}
25[b]	2.44×10^{-7}	1.41×10^{-8}	5.34×10^{-8}	5.63×10^{-3}

[a] Obtained from a nonlinear least-squares fit of the rate data (Fig. 3) to Eq. (2).
[b] Extrapolated from E_a and log$A$ given in Table III.

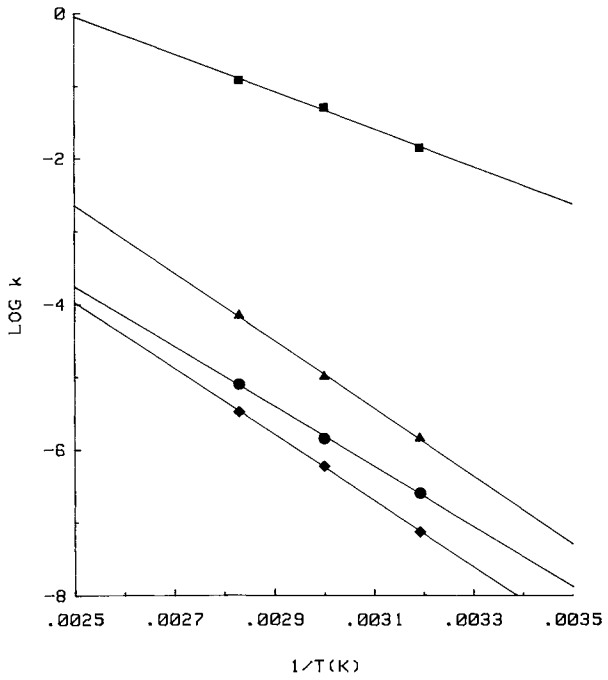

Fig. 4. Arrhenius plots of the degradation of 1. The rate constants k_o (▲), k'_o (◆), k''_o (●), and k_{OH} (■) are taken from Table II.

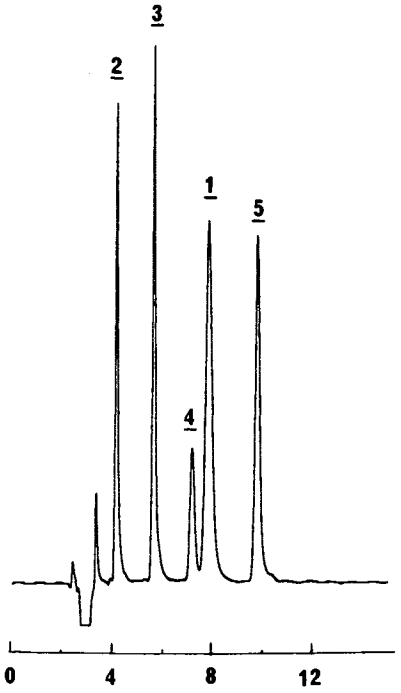

Fig. 5. A HPLC chromatogram showing the separation of degradation products 2–5 from the drug peak 1.

product 5 is predominant (>93%), with the formation of small amounts of the hydrolysis product 2 (<3%) and its cyclized diketopiperazine analogue 3 (<2%). This result indicates that intramolecular cyclization is responsible for most of the two observed water- or neutral-catalyzed kinetic processes (k_o and k'_o).

Intramolecular cyclization leading to the formation of diketopiperazine between the two neighboring amino acids has recently been recognized as an important degradation pathway for peptides (6–8). The diketopiperazine thus formed, however, can further react at a comparable rate at one of the two amide bonds. This amide hydrolysis often complicates the dipeptide reaction kinetics because of the regeneration of the dipeptide and formation of its inverted analogue (8,9).

The degradation leading to the formation of diketopiperazine 5, on the other hand, remains first-order down to 3% remaining (Fig. 2). Further, excellent mass balance was accounted for by products 2, 3, and 5 at pH levels below 4, indicating the absence of an inverted 1 as a significant product. The hydrolysis of the two amide bonds in 5 is therefore insignificant under our reaction conditions. One possible reason for the lack of observing a reversible reaction under our conditions could be that intramolecular cyclization of 1 is greatly facilitated by the favorable conformation resulting from the isoquinoline structure, which prohibits the free rotation of the carboxylic functional group as enjoyed in a simple dipeptide. Although no quantitative kinetic data are available in the literature for comparison with our kinetic data, the common use of severe conditions (temperature >110°C) necessary for studying the cyclization reaction of peptides (7–9) seems to support our suggestion.

According to Scheme I, the major species present in aqueous solution at pH levels below 4 are 1c and 1z. The ammonium functional groups in these two species are not nucleophilic and therefore do not attack the carboxylic acid. The tautomers 1c′ and 1z′ are probably the reactive intermediates for the two neutral- or water-catalyzed processes, k_o and k'_o, respectively (Scheme III). A similar tautomer has been suggested in the acid-catalyzed cyclization of 3-(2-aminophenyl)propionate to the corresponding lactam (10). The detailed reaction pathways after the initial attack as well

Table III. Summary of Activation Parameters for the Degradation of 1 in Aqueous-Solution

Rate constant	E_a (kcal mol^{-1})	log$A$	$\Delta H‡$ (kcal mol^{-1})	$\Delta S‡$ (cal mol^{-1} K^{-1})
k_0	21.3 ± 0.57	9.0 ± 0.38	20.7 ± 0.56	−19.4 ± 1.2
k'_0	20.8 ± 0.31	7.4 ± 0.21	20.7 ± 0.31	−26.8 ± 1.3
k''_0	18.9 ± 0.65	6.6 ± 0.43	18.2 ± 0.64	−30 ± 3.6
k_{OH}	11.8 ± 0.91	6.4 ± 0.60	11.2 ± 0.92	−31 ± 5.5

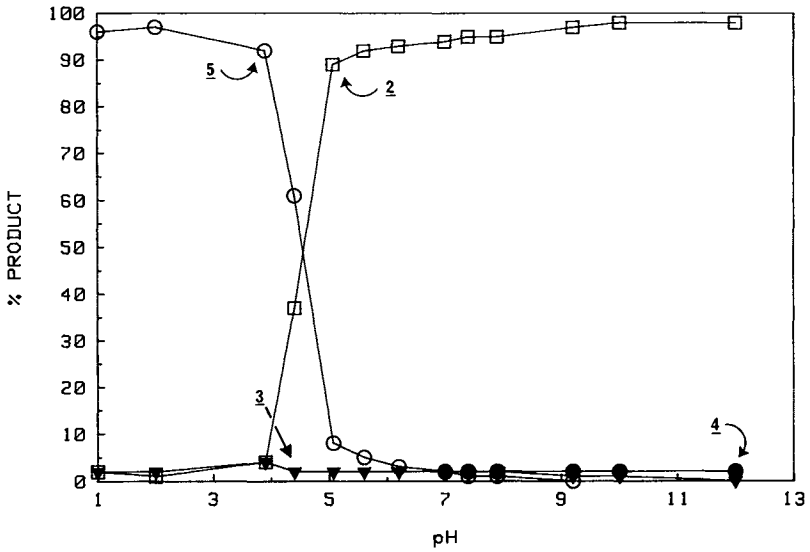

Fig. 6. The distribution of the degradation of products 2–5 as a function of pH at 40°C and ~50% remaining determined by HPLC response factors.

as the rate-determining step of the cyclization process cannot be elucidated with the present data.

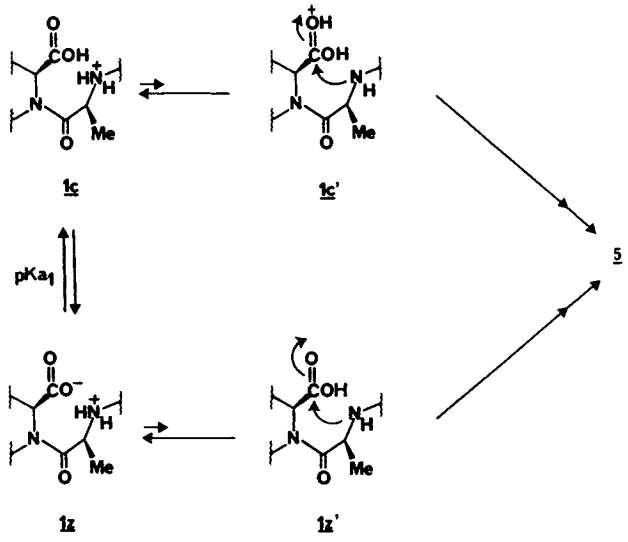

Scheme III

The small amount of ester hydrolysis product observed at pH 4 or below probably comes from specific-acid catalyzed hydrolysis of esters (11). The minor product 3 at pH 4 or below must have come from a secondary reaction(s), i.e., hydrolysis of 5 and/or cyclization of 2. Attempts to resolve these mechanisms through product distribution–time course profiles (not shown) from degraded solutions at pH levels below 4, however, were inconclusive due to the small quantity of 3 formed at different time points.

As the pH increases from 3.5 to 5, hydrolysis product 2 becomes more predominant and eventually accounts for ≥93% of the total products at pH levels above 5 (Fig. 6). This result indicates a change in degradation pathways from cyclization to hydrolysis at pH levels of about 4 to 5. The neutral- or water-catalyzed (k'_o) and specific base-catalyzed (k_{OH}) kinetic processes [Eq. (2)] observed at pH levels above 5 can be attributed to hydrolysis of **1a**. However, to account for the significant k''_o term observed at pH levels

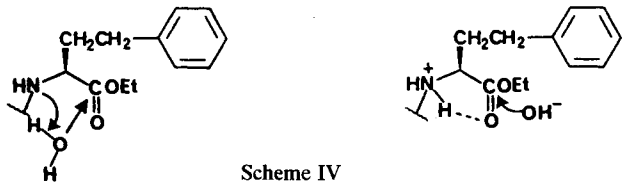

Scheme IV

between 6 and 9 (Fig. 3) and for the decrease in hydrolysis rate at pH levels below pKa_2, an intramolecular general base catalysis from the amino group onto the water molecule is suggested (Scheme IV).

The intramolecular general base catalysis, however, is not available for **1z** where the amino group is positively charged. Alternatively, a kinetically equivalent process involving an intramolecular general acid-specific base catalysis from the ammonium functionality of **1z** can be suggested (12). This would indicate that the hydrolysis reaction is actually controlled by two respective specific base-catalyzed processes for **1z** and **1a**. Again, the present data do not allow the distinction between these two mechanisms.

At pH levels above 7, a small amount (<3%) of the S,S,R drug stereoisomer **4** was detected by HPLC, indicating epimerization at the third chiral center (counting from left to right) in the basic region. A qualitative comparison of the relative acidity of the protons at the three chiral centers provides some insight for the observed specificity in epimerization. At pH levels above 7 the proton at the first chiral center is expected to be the least acidic because it is the only proton among the three that is next to an acid-weakening group, a carboxylate (13). The proton at the second chiral center is adjacent to two acid-strengthening groups (i.e., an amine and an amide) and a neutral methyl group. All three groups attached to the third chiral center, on the other hand, are acid-strengthening groups. The α-ester at the third chiral center is a stronger acid-strengthening group than the amide

(13) at the second chiral center and the γ-phenyl group has yet a slightly more positive effect on the acidity at the third chiral center than the methyl at the second. The proton *at the third chiral center* therefore should be the most acidic, thus giving the observed specificity in epimerization.

CONCLUSION

Through detailed kinetic and product analysis the major degradation mechanisms of **1** in aqueous solution were identified. The two *p*Ka's of **1** appeared to be strongly related to each other and controlled the relative importance of the degradation pathways. Diketopiperazine and diacid drug forms were also found to be the major degradation products for enalapril maleate granulations and tablets (14). Thus, the aqueous stability results revealed in this study may be applied to other ACE inhibitors possessing a similar dipeptide structure (1).

ACKNOWLEDGMENTS

The authors would like to thank Drs. D. M. Johnson and T.-W. Chan for the helpful discussions.

REFERENCES

1. M. J. Wyvratt and A. A. Patchett. *Med. Res. Rev.* 5:485–531 (1985).
2. M. A. Weber and R. M. Zusman. *Drug Ther.* 43–54 (1986).
3. V. J. Dzau. *Drug Ther.* 57–68 (1986).
4. A. Albert and E. P. Serjeant. *Ionization Constants of Acids and Bases,* John Wiley and Sons, New York, 1962, p. 51.
5. A. Albert and E. P. Serjeant. *The Determination of Ionization Constants,* 2nd ed., Chapman and Hall, London, 1971, p. 7.
6. P. R. Bevington. *Data Reduction and Error Analysis for the Physical Sciences,* McGraw-Hill, New York, 1969.
7. S. Steinberg and J. L. Bada. *Science* 213:544–545 (1981).
8. S. M. Steinberg and J. L. Bada. *J. Org. Chem.* 48:2298–2300 (1983).
9. A. A. Brewerton, D. A. Long, and T. G. Truscott. *Trans Faraday Soc.* 66:2297–2304 (1970).
10. B. P. Camilleri, R. Ellul, A. Kirby, and T. G. Mujahid. *J. Chem. Soc. Perkin Trans.* II:1617–1620 (1979).
11. E. K. Euranto. In S. Oatai (ed.), *The Chemistry of Carboxylic Acids and Esters,* John Wiley & Sons, Wiley, 1969, pp. 505–588.
12. H. Bundgaard and E. Falch. *Int. J. Pharm.* 23:223–237 (1985).
13. D. D. Perrin, B. Dempsey, and E. P. Serjeant. *pKa Prediction for Organic Acids and Bases,* Chapman and Hall, London, 1981, pp. 21–43.
14. P. K. Shiromant and J. F. Bavitz. *Drug Dev. Ind. Pharm.* 12:2467–2480 (1986).